RSC Advances

PAPER

View Article Online
View Journal | View Issue

Check for updates

Cite this: *RSC Adv.*, 2019, **9**, 7890

Removal of Pb(II) and Cd(II) from wastewater using arginine cross-linked chitosan–carboxymethyl cellulose beads as green adsorbent

Kaiser Manzoor,[a] Mudasir Ahmad,[b] Suhail Ahmad[a] and Saiqa Ikram *[a]

A one pot approach has been explored to synthesize crosslinked beads from chitosan (CS) and carboxymethyl cellulose (CM) using arginine (ag) as a crosslinker. The synthesized beads were characterized by FTIR, SEM, EDX, XRD, TGA and XPS analysis. The results showed that CS and CM were crosslinked successfully and the obtained material (beads) was analyzed for adsorption of Cd(II) and Pb(II) by using batch adsorption experiments; parameters such as temperature, contact time, pH and initial ion concentration were studied. Different kinetic and thermodynamic models were used to check the best fit of the adsorption data. The results revealed that the kinetics data of the adsorption of Pb(II) and Cd(II) ions shows the best fit with the pseudo second order model whereas the thermodynamics data shows the best fit with the Langmuir isotherm with maximum adsorption capacities of 182.5 mg g^{-1} and 168.5 mg g^{-1} for Pb(II) ions Cd(II) ions, respectively. For the recovery and the regeneration after the one use of the beads, several adsorption–desorption cycles were carried out to check the reusability and recovery of both the metal ion and the adsorbent without the loss of maximum adsorption efficiency.

Received 15th January 2019
Accepted 28th February 2019

DOI: 10.1039/c9ra00356h

rsc.li/rsc-advances

Open Access Article. Published on 11 2019. Downloaded on 2024/7/20 06:15:29.
This article is licensed under a Creative Commons Attribution-NonCommercial 3.0 Unported Licence.

Introduction

Industrialization and advancement in other technologies such as fertilizers for agriculture, antibiotics for healthcare and the setup of various industries on the banks of water bodies have led to increased discharge of pollutants into water bodies.[1,2] These pollutants range from dyes from textile industries, to heavy metal ions from tanning, paint manufacturing, and electroplating industries.[3,4] Exposure to heavy metal ions can cause serious complications in all living creatures, especially in humans. WHO have rightly proposed that some of the prominent chemical concerns of public health are due to heavy metals including cadmium, lead, and mercury. Toxicity due to these three heavy metals often proves fatal and they are also probable human carcinogens.[5–7] In children overexposure to lead causes swelling of the optic nerve (papilledema), ataxia, brain damage (encephalopathy), convulsions, seizures, and impaired consciousness whereas in adults it causes high blood pressure, damage to the reproductive organs, fever, headaches, fatigue, vomiting, anorexia, abdominal pain, constipation, joint pain, incoordination, insomnia, irritability, altered consciousness, and hallucinations. Exposure to cadmium leads to headaches, fatigue, vomiting, nausea, diarrhea, abdominal cramps, emphysema, pulmonary edema, low levels of iron within the red blood and breathlessness (dyspnea).[8,9]

There have been continuous efforts from researchers throughout the world on the removal of heavy metal ions through physical and chemical methods.[10] A large number of techniques such as chemical precipitation, flocculation, reverse osmosis, electrodialysis, membrane filtration, and adsorption have been introduced for remediation of heavy metal ion containing wastewater.[11–14] Among all these techniques adsorption is most efficient and advanced method for being cost efficient and environment friendly. Adsorption of the heavy metal ions using renewable biopolymers and their modified forms is one of the most advancement in adsorption methodology.[15–18] Biopolymers for being environment friendly, biocompatible and biodegradable resources have recently been evaluated for their adsorption characteristics due to presence of ample number of N and O containing functional groups which in turn have higher affinity for heavy metal ions. Chitosan and its derivatives have been extensively studied for adsorption of heavy metal ions from wastewater. Different ways are being proposed for modification of the biopolymers to enhance their adsorption efficiency, cost efficiency, environment friendliness and as well as their reusability. Graft copolymerization of the biopolymers, composites with inorganic/organic hybrid materials and direct functionalization of the polymeric backbone have been used for syntheses of different adsorbent material.[19–26] The important aspect for the adsorption application are: selectivity, capacity, regeneration ability, kinetics, thermodynamics, and the cost efficiency. The use of biopolymers as

[a]*Biopolymer Research Laboratory, Department of Chemistry, Jamia Millia Islamia, New Delhi, India. E-mail: sikram@jmi.ac.in*

[b]*Applied Chemistry, School of Natural & Applied Science, Northwestern Polytechnical University, P. R. China*

This journal is © The Royal Society of Chemistry 2019

Open Access Article. Published on 11 2019. Downloaded on 2024/7/20 06:15:29.
This article is licensed under a Creative Commons Attribution-NonCommercial 3.0 Unported Licence.

adsorbents is common, but the increase in surface area, mechanical properties, and decrease in the swelling is still a challenge.

With the above goal, we have synthesized beads from CS and CM using arginine as crosslinker. Arginine has guanidine moiety which has very high affinity for metal ions due to presence of large number of amine groups. Incorporation of arginine into chitosan/carboxymethyl cellulose increases the adsorption of these macromolecules enormously. The synthesized beads with large surface area and less swelling, showing high removal efficiency demonstrated excellent reusability for removal of these metal ions from aqueous solution. The beads were further evaluated for the soil degradability and began to decompose within five weeks from burying under the soil. The synthesized beads of CS-ag-CM can prove highly efficient adsorbent for removal of Pb(II) and Cd(II) from wastewater.

Material and methods

General remarks

All the chemicals and solvents were purchased from Himedia and Fischer Scientific New Delhi, India Limited. Chitosan (degree of deacetylation $\geq$ 75%) and carboxymethyl cellulose (low viscosity) were used. Double distilled water was used throughout the experiment. FTIR was recorded on Bruker Tensor 37 Spectrophotometer (Central Instrumentation Facility, Jamia Millia Islamia New Delhi, India) by scanning the product in the wavelength range from 4000 cm^{-1} to 500 cm^{-1}. SEM imaging was carried out using FEI Quanta 200 FESEM (50–50k×) University Sophisticated Instruments Facility (USIF) and TGA was performed on TG-A6300 instrument (SII Nano Technology Inc. Tokyo, Japan) Department of Chemistry, Aligarh Muslim University Aligarh, India. XRD analysis was done on D8 Advance diffractometer (Bruker) (Central Instrumentation Facility, Jamia Millia Islamia New Delhi, India) with Cu target λ = 0.154 nm at 40 kV, and 2θ was 10°–80°. Batch adsorption was used to carry out the adsorption studies. XPS was performed on ESCA+, (Omicron Nanotechnology, Oxford Instrument Germany, Al kα radiation $h\nu$ = 1486.7 eV) at Materials Research Centre Malviya National Institute of Technology JLN Marg, Jaipur, India 302017.

Preparation of arginine crosslinked CS/CM adsorbent

Chitosan solution was prepared by dissolving 3 g (6×10^{-3} moles) of CS in 0.01 M acetic acid solution. CMC solution was prepared by dissolving 1.57 g (6×10^{-3} moles) and arginine solution was prepared by dissolving 2 g (1.2×10^{-2} moles) in double distilled water. Chitosan solution was added simultaneously to flask containing CM and arginine solutions. On the dropwise addition of the chitosan solution the solid bead structures are formed while the mixture was continuously stirred at 110–120 °C for 1 h. The resultant product was obtained as bead like structures, washed with distilled water till solution stabilises at neutral pH. Ethanol was added to remove the water and left for drying in oven at 40 °C for 24 h.

Procedure for metal ion adsorption

Metal ion solutions of Pb(II) and Cd(II) ion were prepared by dissolving desired amount of salts of these metal ions in double distilled water. Batch adsorption method was used for analyzing the effect of dosage, pH, initial ion concentration, contact time and temperature on the adsorption of the metal ions onto CS-ag-CM. All the batch adsorption methods to study the kinetics and thermodynamics of adsorption of Pb(II) and Cd(II) ions from aqueous solution were performed thrice in order to obtain the precise values for different adsorption quantities. The amount of metal ion adsorbed on the adsorbent was obtained by using eqn (1)

$$q = \frac{C_o - C_e}{m} \times V \quad (1)$$

where q is the adsorption capacity in mg g^{-1}, C_o and C_e (mg L^{-1}) are the initial and final metal ion concentrations respectively, V (L) is the volume of the solution taken and m (g) is the mass of the adsorbent spent.

Procedure for metal ion desorption

The metal ion adsorbed CS-ag-CM was placed in the volumetric conical flasks containing 0.01 M EDTA solution and was stirred in an orbital shaker for about one hour and readings were noted down every 10 min until desorption was complete. The beads were washed with water and dried in oven for their repetitive use.

Swelling studies

The swelling studies of CS, CM, and CS-ag-CM were carried out in acidic, neutral and alkaline solutions at 298 K. The extent of swelling was obtained by using equation

$$\% \text{ swelling} = \frac{w_s - w}{w} \times 100 \quad (2)$$

where w_s is the swollen weight of the material whereas w is the dry weight of the material.

Results and discussions

Preparation of arginine crosslinked chitosan/carboxymethyl cellulose beads

The covalent bonding of arginine with both CS and CM requires esterification or amidation of the carboxyl group of ag or CM with the amine group on CS and ag.[27] Esterification although less dominant than amidation due to its reversible nature is favored at lower temperature however amide bond is formed at higher temperature because of the initial protonation of the $-NH_2$ group. The product CS-ag-CM obtained consists of both ester and amide linkages as can be shown from the FTIR spectrum of the product (Scheme 1).

Characterization of CS-ag-CM

The chemical functionalization of cellulose and chitosan with arginine was characterized by FTIR, XRD, SEM. The FTIR spectrum of CS Fig. 1 shows band at 3600–3300 cm^{-1} which can

Open Access Article. Published on 11 2019. Downloaded on 2024/7/20 06:15:29.
This article is licensed under a Creative Commons Attribution-NonCommercial 3.0 Unported Licence.

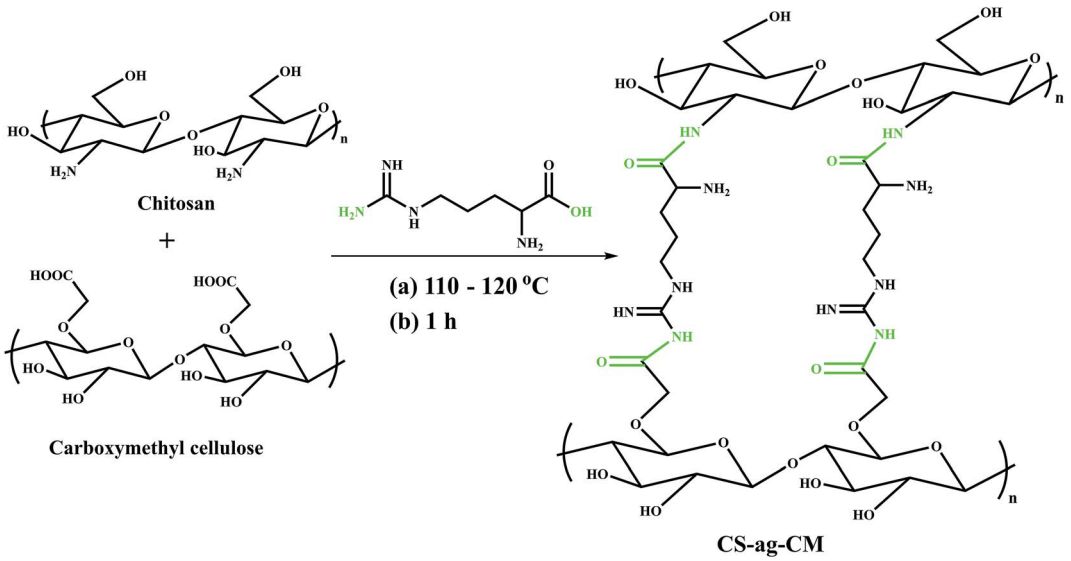

Scheme 1 Reaction pathway.

be assigned to –N–H stretching vibration overlapped with O–H stretch, while the bands at 1652 cm^{-1}, 1550 cm^{-1} arise due to carbonyl group of amino acetyl moiety and –N–H bending vibrations respectively.[28] The spectrum of CM shows the characteristic bands at 3400 cm^{-1}, 1590 cm^{-1}, 1405 cm^{-1} which are assigned to O–H bending, C=O stretching of carboxyl and C–H bending respectively.[29] The crosslinked adsorbent CS-ag-CM shows characteristic peak at 1746 cm^{-1} and 1650 cm^{-1} which can be assigned to the C=O stretching frequencies of ester and amide carbonyls, respectively. Furthermore, the bands appearing at 1152 cm^{-1} and 899 cm^{-1} are characteristic of glycosidic bridge of the amide bond. The absorption band appearing at 1372 cm^{-1} is due to C–N stretching vibrations.[30–32]

XRD patterns of the CS, CM, and CS-ag-CM are shown in Fig. 2. The less intense broad peaks of CS and CM at $2\theta = 20°$ are the characteristic of the amorphous nature of these polymers. However, the sharp and intense peat at $2\theta = 20°$ of CS-ag-CM shows the transformation towards more crystalline nature of the CS-ag-CM which is typically attributed to the crosslinking of the two polymeric backbones by arginine.

SEM micrographs of CS, CM, CS-ag-CM and M-CS-ag-CM [M = Cd(II), Pb(II)] are shown in Fig. 3(a–e). As predictable from the

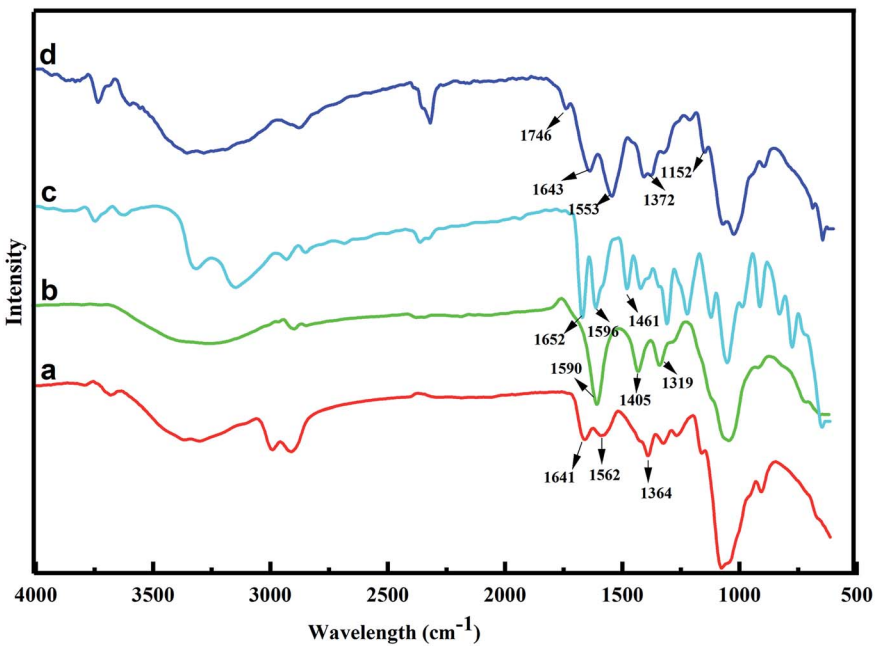

Fig. 1 FTIR spectrum of (a) CS, (b) CM, (c) ag and (d) CS-ag-CM.

This journal is © The Royal Society of Chemistry 2019

Open Access Article. Published on 11 2019. Downloaded on 2024/7/20 06:15:29.
This article is licensed under a Creative Commons Attribution-NonCommercial 3.0 Unported Licence.

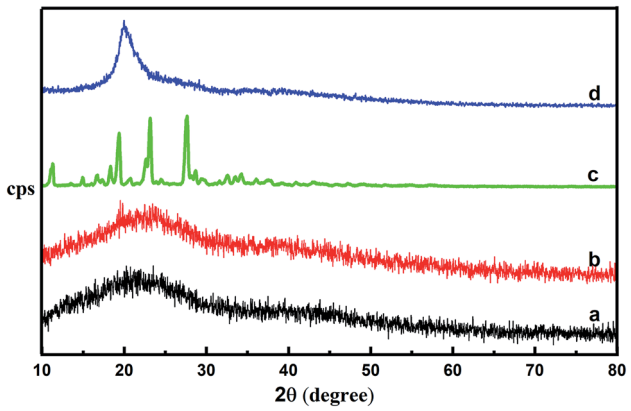

Fig. 2 XRD patterns of (a) CS, (b) CM, (c) ag and (d) CS-ag-CM.

SEM images (Fig. 3a and b) of both CS and CM, their surfaces are smooth and non-porous, their XRD data revealing their amorphous structure. The XRD pattern of pure arginine (ag) shows the absolute crystalline structure with distinct peaks. The surface morphology of the adsorbent (Fig. 3c) CS-ag-CM shows the porous surface with large number grooves and increased surface area. The surface of CS-ag-CM after adsorption of Pb(II) ions white spots (Fig. 3e and f) can be seen on the surface of adsorbent. On increasing the magnification of the Pb(II) ion adsorbed surface further, covered surface of CN-ag-CM is clearly indicative of Pb(II) covered surface.

Thermal analysis

Thermal analysis of all the raw material and the final product were carried out in order to evaluate the thermal stability of the

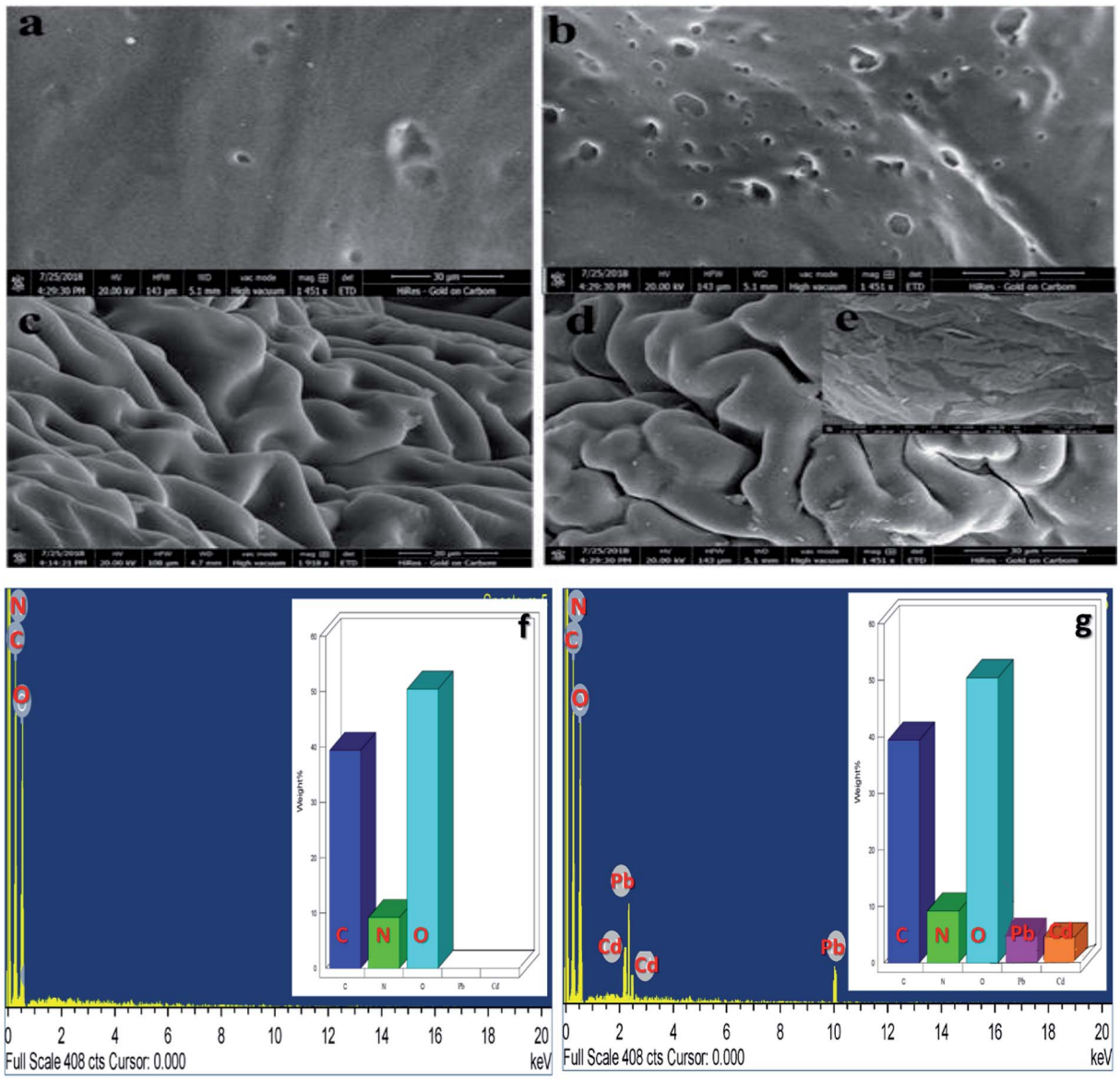

Fig. 3 SEM micrographs of (a) CS, (b) CM, (c) CS-ag-CM, (d) Pb(II)/Cd(II)-CS-ag-CM (e) Pb(II)/Cd(II)-CS-ag-CM and EDX spectrum of (f) CS-ag-CM and (g) Pb(II)/Cd(II)-CS-ag-CM.

Open Access Article. Published on 11 2019. Downloaded on 2024/7/20 06:15:29.
This article is licensed under a Creative Commons Attribution-NonCommercial 3.0 Unported Licence.

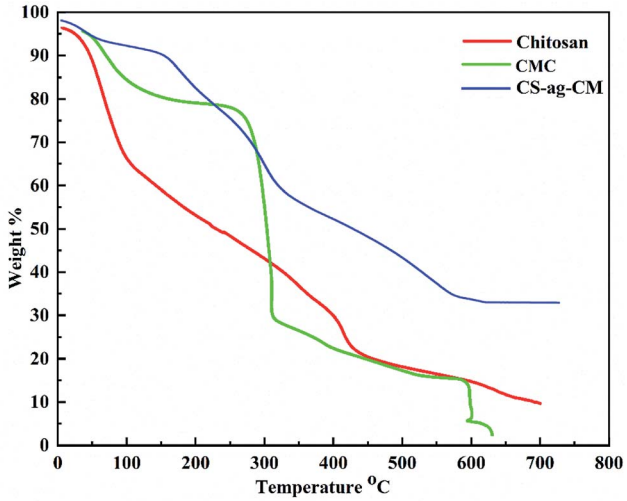

Fig. 4 TGA of CS, CM and CS-ag-CM.

adsorbent as shown in Fig. 4. It was observed that the adsorbent CS-ag-CM was thermally more stable than both CS and CM. The amount of the residual CS-ag-CM is much larger than the CS and CM at 600 °C which is approximately 45%, is the strong evidence for the crosslinking of CS and CM in presence of AG, already confirmed by FTIR and XRD analyses.

XPS analysis

XPS analyses shows the evidence of the adsorption of Pb(II) and Cd(II) on to CS-ag-CM as shown in Fig. 5. The adsorption of Pb species with the appearance of new peaks in the range of 136 and 410 eV correspond to Pb 4p and Pb 4d respectively. The spin–orbit components ($\Delta_{metal} = 4.9$ eV) in the Pd 4f region with binding energy of Pb $4f_{7/2}$ 138.9 eV are characteristic of Pb(II) species. Similarly, the peaks at 406 and 643 eV correspond to Cd 3d and Cd 3p species of Cd(II) respectively. These results confer that (i) both Pb(II) ions and Cd(II) ions are not reduced to metallic forms upon contact with the CS-ag-CM beads, and (ii)

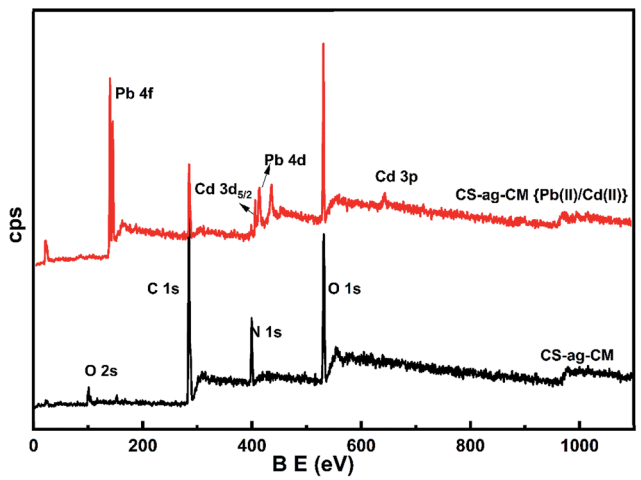

Fig. 5 XPS of CS-ag-CM before and after adsorption of Pb(II) and Cd(II).

the adsorption results from the coordination of Pb(II) and Cd(II) species by the guanidine moiety of the crosslinker arginine.[33,34]

Adsorption studies

Adsorption parameters were calculated using equilibrium batch adsorption method. A series of 50 ppm, 100 ppm, 150 ppm and 200 ppm concentration solutions of Pb(II) and Cd(II) ions from their respective salts were prepared and effect of different parameters on adsorption process such as temperature, contact time, pH, initial ion concentration were observed, and relative conclusions were made on comparing the obtained quantities. It was observed that the adsorption capacity for uptake of Pb(II) ions was 182.5 mg g^{-1} and that for Cd(II) ions was 168.5 mg g^{-1} from the aqueous solution.

Effect of temperature. In order to study the effect of temperature on adsorption of Pb(II) and Cd(II) 50 ppm solution of both these metal ions was taken in two different flasks, 100 mg of adsorbent was added to both the flasks and left in orbital shaker for 1 h each at 303 K. The solutions were filtered, and the remaining concentration was determined by titration, similar procedure was repeated at temperatures. From the plot of q_e *vs.* T Fig. 6(a), it was observed that initially the adsorption increased on increasing with temperature with maximum adsorption at 310 K for Cd(II) and 315 K for Pb(II) ions and there on decreases with further increase in temperature. This can be attributed to the fact that initially when temperature increases the thermal energy of the metal ions also increases which in turn increase the probability of contact between the vacant sites of the adsorbent and the metal ions. However, on increasing the temperature further the thermal vibration of metal ions become much faster than the adsorbent–metal ion interaction resulting in the release of metal ions back into the solution.

Effect of pH. Effect of pH on adsorption of Cd(II) and Pb(II) onto CS-ag-CM was studied by preparing 50 ppm solution of metal ions with different pH and were subjected to shaking in orbital shaker for 1 h at temperatures 310 K for Cd(II) and 315 K for Pb(II) ions. The resultant solutions were filtered after 1 h and the remaining concentration was determined by titration. The graph of q_e *vs.* pH (Fig. 6(b)) shows that initially the amount of Cd(II) and Pb(II) adsorbed onto CS-ag-CM increases with increase in the pH both attaining maxima at pH = 6.5. With further increase in pH, net adsorption of metal ions onto adsorbent does not increase because of the formation of metal hydroxides in alkaline medium. At lower pH, adsorption is not prominent due to higher concentration of H^+ ions which competes with Cd(II) and Pb(II) ion adsorption onto CS-ag-CM.[35,36]

Effect of contact time. Contact time between the adsorbent surface and the adsorbate molecules has a profound effect on the adsorption capacity. Initially when all the adsorbent sites are vacant, the adsorbate molecule adhere to the vacant sites as soon as the metal ions come in contact with them thereby showing a gradual increase in the adsorption with time till a maximum is attained at 40 min as shown in Fig. 6(c). Thereafter no further increase in adsorption is seen which occurs due to fact that when all the adsorbent sites are occupied a dynamic

 This journal is © The Royal Society of Chemistry 2019

Open Access Article. Published on 11 2019. Downloaded on 2024/7/20 06:15:29.
This article is licensed under a Creative Commons Attribution-NonCommercial 3.0 Unported Licence.

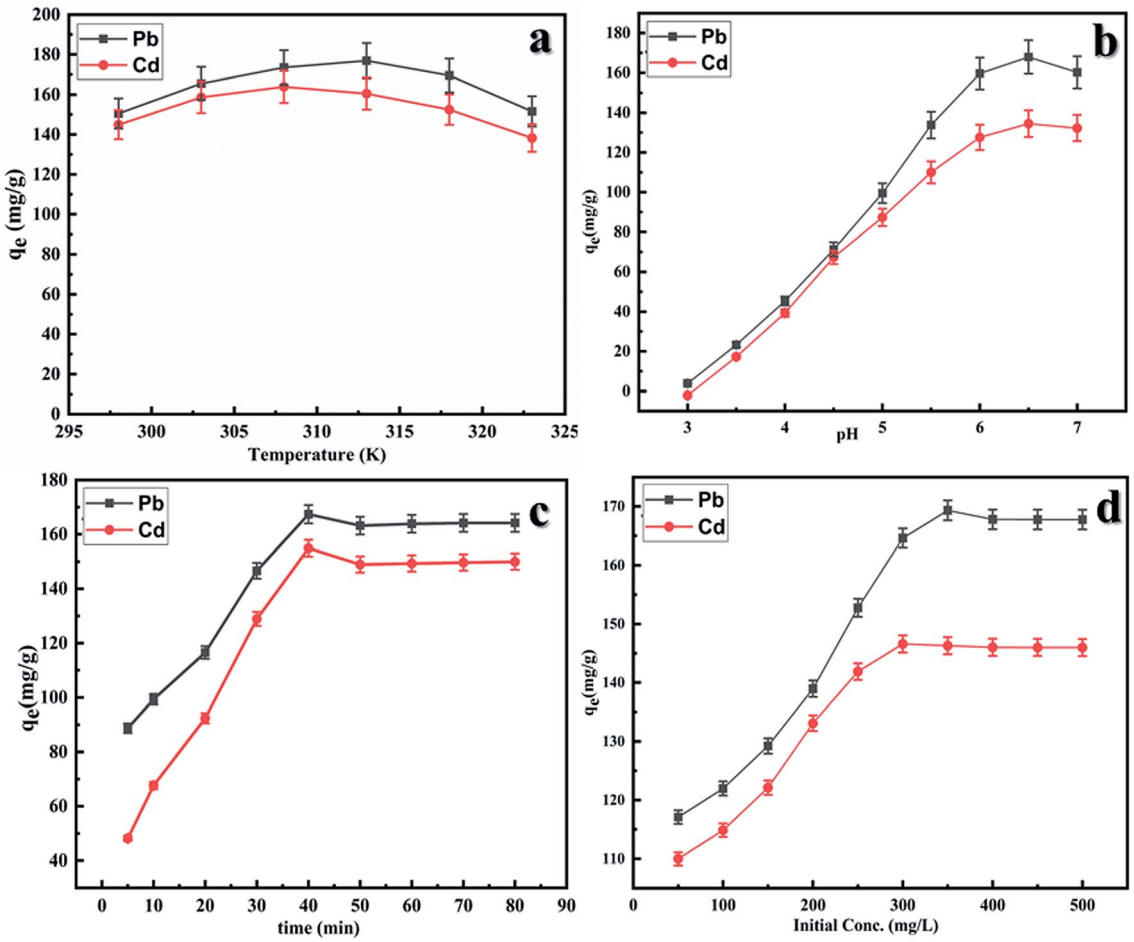

Fig. 6 Effect of (a) temperature, (b) pH, (c) contact time and (d) initial ion concentration on the adsorption of Pb(II) and Cd(II) onto CS-ag-CM.

equilibrium is attained in which the number of molecules being adsorbed equals the number of adsorbate molecules being desorbed.[37,38]

Effect of initial concentration. Initial concentration of the adsorbate molecules affects the rate of adsorption to a great extent as depicted in Fig. 6(d). At the lower initial adsorbate concentration lesser number of collisions occur between the adsorbate molecules and the adsorbent which increase with increase in the initial adsorbate concentration and shows sharp increase in the adsorption capacity up to initial concentration of 300 mg L^{-1} for Cd(II) ion and 325 mg L^{-1} for Pb(II) ion. There is no further increase in adsorption with increasing initial ion concentration due to attainment of the dynamic equilibrium between free adsorbate ions in solution and adsorbed metal ions.[39]

Adsorption kinetics. In order to determine the rate of adsorption of Pb(II) and Cd(II) onto adsorbent, three different kinetic models were used, pseudo first order, pseudo second order and intraparticle diffusion model.[39–44] The linear forms of these models are given below:

$$\ln(q_e - q_t) = \ln q_e - k_1 t \quad (3)$$

$$\frac{t}{q_t} = \frac{1}{k_2 q_e^2} + \left(\frac{1}{q_e}\right) t \quad (4)$$

$$q_t = K_{id} t^{1/2} + C \quad (5)$$

where q_e and q_t are adsorption capacities at equilibrium and at time t respectively, k_1, k_2 and K_{id} are first order, second order and intraparticle diffusion rate constants respectively. On comparing the R^2 values of the plots obtained from these equations as shown in Fig. 7(a–c), it was observed that pseudo first order plot with $R^2 = 0.990$ (Pb) and 0.944 (Cd) and could not explain the adsorption phenomena. However, pseudo second order model could establish a much better relation in the adsorption kinetics with R^2 values corresponding to 0.999 for both Pb(II) and Cd(II) ions which has much been used to describe the kinetics of divalent metal ions onto peat. The intraparticle diffusion plot shows multilinearity in the adsorption of both Pb(II) and Cd(II) ions which suggests the involvement of different pathways. The first step corresponds to boundary layer diffusion of Pb(II) and Cd(II) ions on to CS-ag-CM while as the second step corresponds to the gradual sorption of these ions onto adsorbent. The intraparticle diffusion of Pb(II) and Cd(II) ions in the second step slows down due to low leftover

Open Access Article. Published on 11 2019. Downloaded on 2024/7/20 06:15:29.
This article is licensed under a Creative Commons Attribution-NonCommercial 3.0 Unported Licence.

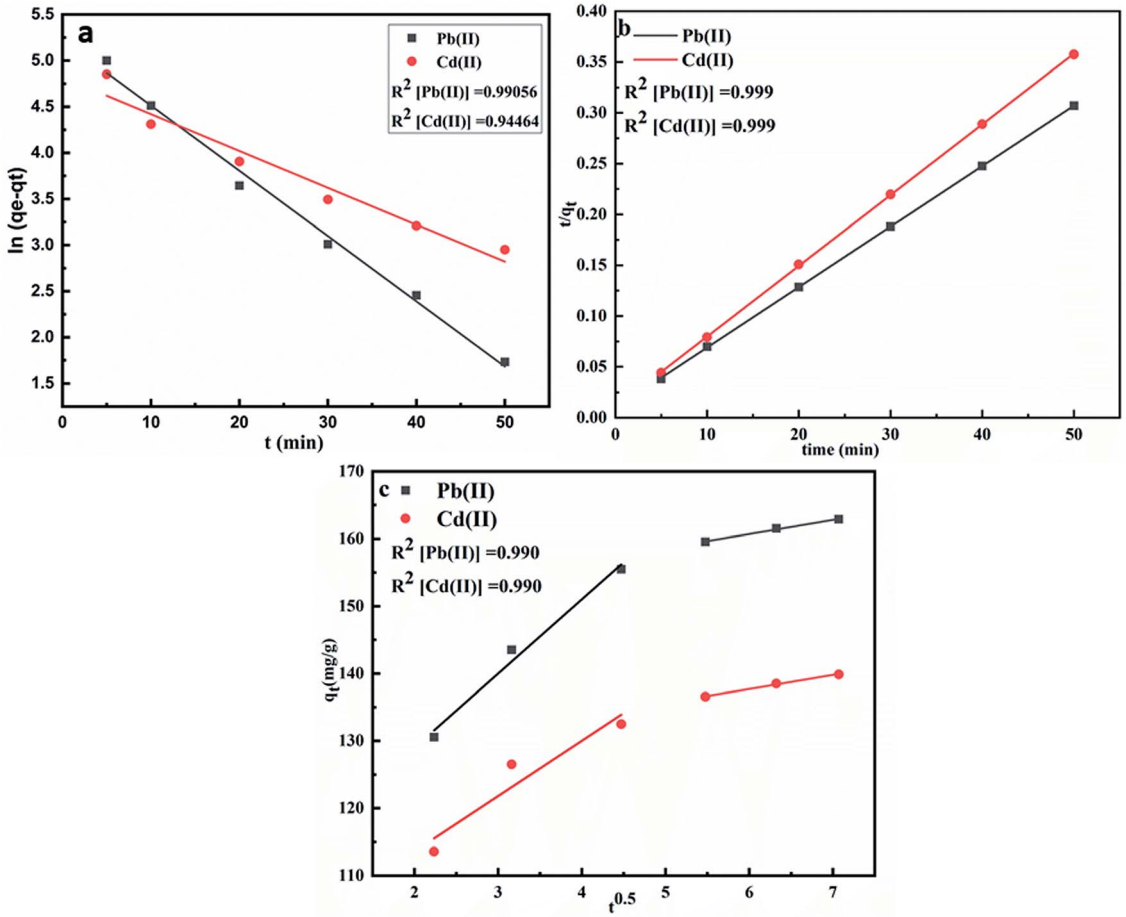

Fig. 7 Plots of (a) pseudo first-order kinetics, (b) pseudo second order kinetics and (c) intraparticle diffusion model.

concentration of these ions in the solution the similar adsorption behaviour shown in the adsorption of Pb(II) ions onto sawdust and polyacrylamide zirconium(IV) iodate (Table 1).[45]

Adsorption isotherms. Adsorption isotherms are used to establish the relation between the amount of adsorbate adsorbed and the unadsorbed adsorbate. There are a number of adsorption isotherms but most important being Langmuir isotherm, Freundlich isotherm, and Temkin isotherm and their linear forms as shown below:[46]

$$\frac{1}{q_e} = \left(\frac{1}{K_L q_m}\right)\frac{1}{C_e} + \frac{1}{q_m} \quad (6)$$

$$\ln q_e = \frac{1}{n}\ln C_e + \ln K_F \quad (7)$$

$$q = \frac{RT}{b_T}\ln A_T + \frac{RT}{b_T}\ln C_e \quad (8)$$

where C_e (mg L^{-1}), q_m (mg g^{-1}) and q_e (mg g^{-1}) are the equilibrium concentration, equilibrium adsorption capacity, maximum adsorption capacity respectively. K_L and K_F are Langmuir and Freundlich constants respectively, R (8.314 J K^{-1} mol^{-1}) is gas constant and T (K) is temperature. A_T (L g^{-1}) and b_T (J mol^{-1}) are Temkin constants associated with the heat of adsorption.

The Langmuir model (eqn (6)) is usually used to describe the monolayer adsorption of adsorbate at the surface of adsorbent considering the similar types of adsorbent vacant sides and similar adhesive forces that bind the adsorbate molecules to the

Table 1 Kinetic parameters of pseudo first order, pseudo second order and intraparticle diffusion model for adsorption of Pb(II) and Cd(II) onto CS-ag-CM

	Pseudo first order			Pseudo second order			Intraparticle diffusion model		
	k_1 (g mg^{-1} min^{-1})	q_m (mg g^{-1})	R^2	k_2 (g mg^{-1} min^{-1})	q_m (mg g^{-1})	R^2	K_{id} (mg g^{-1} $min^{1/2}$)	C (mg g^{-1})	R^2
Pb(II)	0.070	185.236	0.990	0.003	181.159	0.999	11.021	106.924	0.971
Cd(II)	0.03998	123.993	0.94464	0.0037	164.744	0.999	5.0281	107.165	0.86013

This journal is © The Royal Society of Chemistry 2019

Open Access Article. Published on 11 2019. Downloaded on 2024/7/20 06:15:29.
This article is licensed under a Creative Commons Attribution-NonCommercial 3.0 Unported Licence.

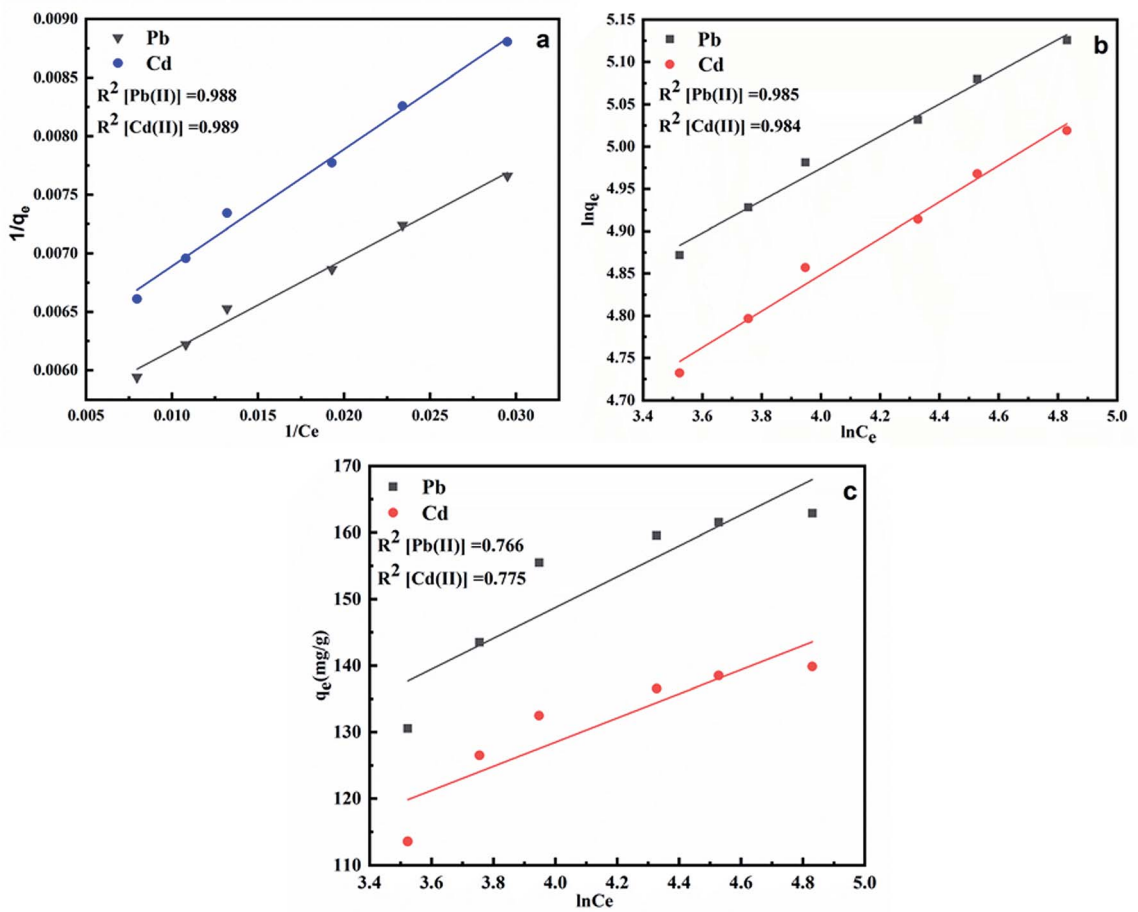

Fig. 8 Isotherm plots of (a) Langmuir isotherm, (b) Freundlich isotherm and (c) Temkin isotherm.

Table 2 Parameters of various isotherm models for adsorption of Pb(II) and Cd(II) onto CS-ag-CM

	Langmuir			Freundlich			Temkin		
	K_L (L mg^{-1})	q_m (mg g^{-1})	R^2	K_F	n	R^2	A_T	b_T	R^2
Pb(II)	6.92×10^{-2}	185.5	0.988	67.49	5.24	0.985	11.23	115.90	0.766
Cd(II)	5.91×10^{-2}	169.7	0.989	53.94	4.64	0.984	21.72	147.92	0.765

adsorbent surface neglecting the interactions between the adsorbate molecules.

Freundlich isotherm (eqn (7)) gives information about the adsorption on heterogeneous surfaces with the possibility of multilayer adsorption while as Temkin isotherm model (eqn (8)) takes in consideration the adsorbate–adsorbent interactions assuming linearity in the evolution of adsorption energy and the surface coverage of the adsorbent.

Langmuir isotherm assumes monolayer coverage on a homogeneous surface with identical adsorption sites studied for gas adsorption on solid surface. However, in solution–solid systems, a lot of factors come into play such as hydration forces, mass transfer *etc.* which makes it more complicated, and obeying the isotherm does not necessarily reflect the validity of assumptions. In such systems the isotherm adequacy can be seriously affected by the experimental conditions, the range of concentration of the solute/adsorbate in particular. Both Langmuir and Freundlich isotherms might adequately describe the same set of liquid–solid adsorption data at certain concentration ranges, particularly if the concentration is small and the adsorption capacity of the solid is large enough to make both isotherm equations approach a linear form.

The plots obtained for the three isotherm models for adsorption of Pb(II) and Cd(II) onto CS-AG-CM are shown in Fig. 8(a–c). All the three models fit the adsorption process of Pb(II) and Cd(II) onto CS-ag-CM to different extent from good to best. The Freundlich model with R^2 values 0.985 for Pb(II) and 0.984 for Cd(II) is less suitable for explaining the adsorption process as compared to Langmuir plot with R^2 0.988 for Pb(II) and 0.989 for Cd(II) which shows the best fit with the adsorption

Open Access Article. Published on 11 2019. Downloaded on 2024/7/20 06:15:29.
This article is licensed under a Creative Commons Attribution-NonCommercial 3.0 Unported Licence.

Table 3 Comparison of the adsorption capacities of various adsorbents for adsorption of Pb(II) and Cd(II) ions from wastewater

Metal Ion	Adsorbent	Q (mg g^{-1})	Reference
Pb^{2+}	Chitosan beads	34.98	47
	Epichlorohydrin-crosslinked chitosan	34.13	48
	Carboxymethylated cellulose	24.59	49
	Chitosan–GLA beads	14.24	47
	Chitosan–GLA–citric acid (C-Gch) flake	76.75 at 20 °C 101.7 at 30 °C 103.6 at 40 °C	50
	γ-Fe_2O_3 nanoparticles	69.0	51
	Chitosan coated calcium alginate	106.9	52
	CS-ag-CM beads	182.5	Present study
Cd^{2+}	Amino functionalized mesoporous silica	18.3	53
	Nano-alumina	83.3	54
	Amino functionalized magnetic graphenes composite	27.8	55
	Polyvinyl alcohol/polyacrylic acid double network gel	115.9	56
	Soy protein hollow microspheres	120.8	57
	CS-ag-CM beads	168.5	Present study

Table 4 Adsorption–desorption parameters for evaluating the reusability of CS-ag-CM

	(%) Adsorbed						(%) Desorbed					
No. of cycles	1	2	3	4	5	6	1	2	3	4	5	6
Pb(II)	92.5	92.8	93.8	94.2	94.6	95.3	97.5	96.8	98.2	99.0	98.5	98.8
Cd(II)	91.5	91.9	92.2	92.6	93.0	93.5	96.5	96.2	96.7	97.0	97.2	96.6

of Pb(II) and Cd(II) onto CS-ag-CM. The isotherm parameters and the regression coefficients of different isotherm models are shown in Table 2. It is clear from the correlation coefficients that Langmuir model best correlates the adsorption of Pb(II) and Cd(II) onto CS-ag-CM with maximum adsorption capacities 185.5 mg g^{-1} for Pb(II) and 169.7 mg g^{-1} for Cd(II) ions obtained from the slope of the plot which is higher than any of the previously synthesized adsorbent for removal of Pb(II) and Cd(II) as shown in Table 3. Furthermore, the higher values of b_T for Pb(II) and Cd(II) suggest the stronger adhesion of these metal ions onto adsorbent surface.

Recycling studies through successive adsorption–desorption cycles

The reusability and stability of the adsorbent was evaluated by subjecting it to several adsorption–desorption cycles. The solutions of 100 ppm each of Pb(II) and Cd(II) were used for adsorption by CS-ag-CM by shaking these solutions in orbital

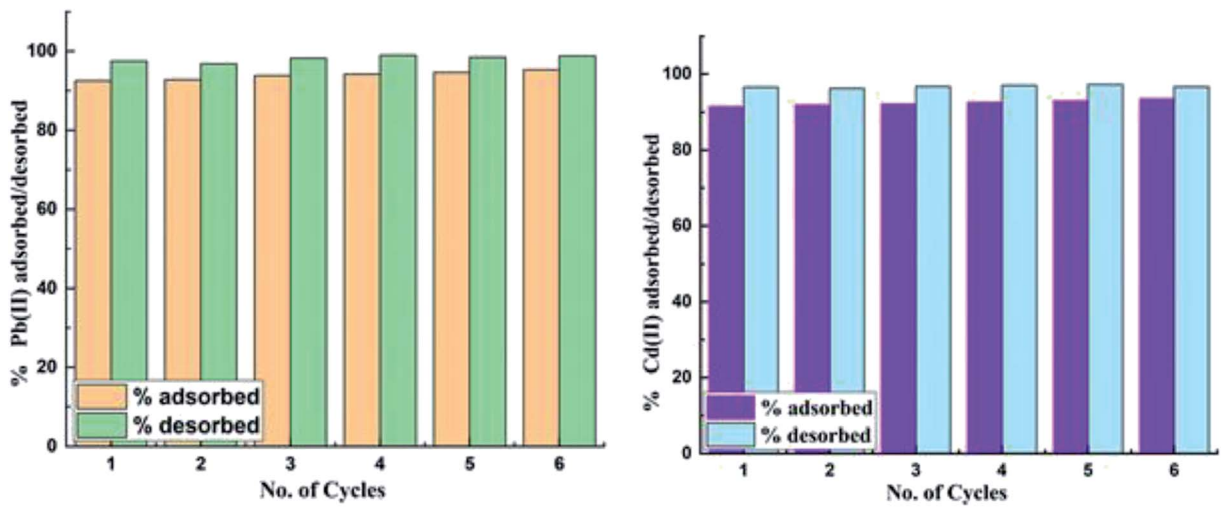

Fig. 9 Percent recovery/regeneration of (a) Pb(II) and (b) Cd(II) from the CS-ag-CM.

 This journal is © The Royal Society of Chemistry 2019

Open Access Article. Published on 11 2019. Downloaded on 2024/7/20 06:15:29.
This article is licensed under a Creative Commons Attribution-NonCommercial 3.0 Unported Licence.

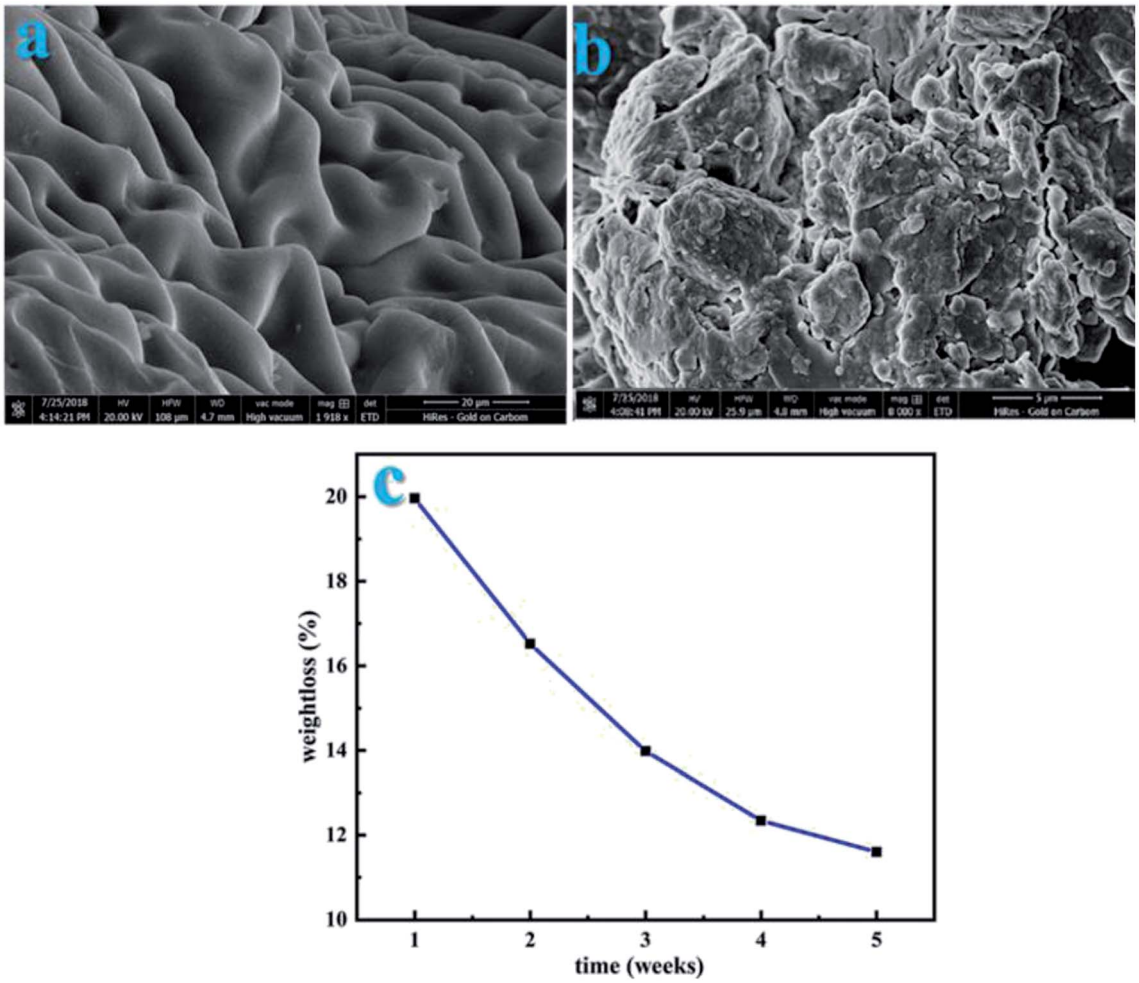

Fig. 10 Soil degradation of the adsorbent before burial (a) CS-ag-CM, (b) CS-ag-CM after burial of five weeks under the soil, and (c) graph showing weight loss of CS-ag-CM for 5 weeks.

agitator at 213 K for 30 min. Thereafter the adsorbent with Pb(II) and Cd(II) adsorbed on its surface was dried and treated with 0.1 M HCl solutions and shaked for 30 min. Six successive adsorption–desorption cycles were repeated until all the metal ions were recovered from the adsorbent. The remaining concentrations were determined by AAS and it was observed that 96% of the dissolved metal ions were recovered (Table 4 and Fig. 9).

Soil degradability test

To analyze the biodegradability of the used adsorbent in the environment, the CS-ag-CM was buried under the soil so as to study its self-decomposition. The SEM images in Fig. 10(a and b) shows the surface morphology of a sample before and after burial Fig. 10(a and b), respectively. The decomposition of the sample was high in the first week due to sufficient availability of oxygen and thereafter slowed down as shown in Fig. 10(c).

Conclusion

The increase in the release of toxic heavy metal ions into the environment is a serious threat to biological life and hence their removal from water is major concern worldwide. In the current work, we have decreased the hydrophilic property of chitosan together with the higher affinity of the guanidine group of the arginine for metal ions for synthesizing the beads for removal of Pb(II) and Cd(II) from aqueous solution. The adsorption efficiency, biodegradability, swelling as well as its reusability for the removal of these heavy metal ions have been evaluated through batch adsorption method and other spectroscopic techniques by applying various kinetic and thermodynamic models. It has been observed that the synthesized beads were able to remove Pb(II) and Cd(II) from aqueous solution with removal efficiency of 95.3% for Pb(II) and 93.5% for Cd(II) which is higher than the adsorbents. The regeneration and the recovery of the crosslinked beads is evaluated first time with the constant adsorption efficiency up to 6 adsorption–desorption cycles. This factor makes the CS-ag-CM as good adsorbent for the adsorption of Pb(II) and Cd(II), as the process need low operational cost and environmentally friendly.

Conflicts of interest

There are no conflicts to declare.

Open Access Article. Published on 11 2019. Downloaded on 2024/7/20 06:15:29.
This article is licensed under a Creative Commons Attribution-NonCommercial 3.0 Unported Licence.

Acknowledgements

Authors acknowledge Central Instrumental Facility and Centre for Nanoscience and Nanotechnology Jamia Millia Islamia New Delhi for providing FTIR and XRD facilities, Indraprastha University New Delhi for providing SEM facility and Aligarh Muslim University for providing EDX and TGA facility. Author also acknowledges MNIT Jaipur for providing XPS facility. Furthermore, the authors declare no financial interests from any funding source.

References

1 D. Tilman, K. G. Cassman, P. A. Matson, R. Naylor and S. Polasky, Agricultural sustainability and intensive production practices, *Nature*, 2002, **418**, 671–677, DOI: 10.1038/nature01014.

2 C. Seiler and T. U. Berendonk, Heavy metal driven co-selection of antibiotic resistance in soil and water bodies impacted by agriculture and aquaculture, *Front. Microbiol.*, 2012, **3**, 399–409, DOI: 10.3389/fmicb.2012.00399.

3 W. S. Wan Ngah, L. C. Teong and M. A. K. M. Hanafiah, Adsorption of dyes and heavy metal ions by chitosan composites: a review, *Carbohydr. Polym.*, 2011, **83**, 1446–1456, DOI: 10.1016/j.carbpol.2010.11.004.

4 D. Gola, A. Malik, M. Namburath and S. Z. Ahammad, Removal of industrial dyes and heavy metals by *Beauveria bassiana*: FTIR, SEM, TEM and AFM investigations with Pb(II), *Environ. Sci. Pollut. Res.*, 2018, **25**, 20486–20496, DOI: 10.1007/s11356-017-0246-1.

5 WHO, *Guidelines for drinking-water quality*, 2011, DOI: 10.1016/S1462-0758(00)00006-6.

6 C. F. Carolin, P. S. Kumar, A. Saravanan, G. J. Joshiba and M. Naushad, Efficient techniques for the removal of toxic heavy metals from aquatic environment: a review, *J. Environ. Chem. Eng.*, 2017, **5**, 2782–2799, DOI: 10.1016/j.jece.2017.05.029.

7 F. Fu and Q. Wang, Removal of heavy metal ions from wastewaters: a review, *J. Environ. Manage.*, 2011, **92**, 407–418, DOI: 10.1016/j.jenvman.2010.11.011.

8 O. E. Orisakwe, The role of lead and cadmium in psychiatry, *N. Am. J. Med. Sci.*, 2014, **6**, 370–376, DOI: 10.4103/1947-2714.139283.

9 M. Jaishankar, T. Tseten, N. Anbalagan, B. B. Mathew and K. N. Beeregowda, Toxicity, mechanism and health effects of some heavy metals, *Interdiscip. Toxicol.*, 2014, **7**, 60–72, DOI: 10.2478/intox-2014-0009.

10 F. Fu and Q. Wang, Removal of heavy metal ions from wastewaters: a review, *J. Environ. Manage.*, 2011, **92**, 407–418, DOI: 10.1016/j.jenvman.2010.11.011.

11 M. Ahmad, K. Manzoor, S. Ahmad and S. Ikram, Preparation, Kinetics, Thermodynamics, and Mechanism Evaluation of Thiosemicarbazide Modified Green Carboxymethyl Cellulose as an Efficient Cu(II) Adsorbent, *J. Chem. Eng. Data*, 2018, **63**, 1905–1916, DOI: 10.1021/acs.jced.7b01008.

12 M. Ahmad, K. Manzoor, R. R. Chaudhuri and S. Ikram, Thiocarbohydrazide Cross-Linked Oxidized Chitosan and Poly(vinyl alcohol): A Green Framework as Efficient Cu(II), Pb(II), and Hg(II) Adsorbent, *J. Chem. Eng. Data*, 2017, **62**, 2044–2055, DOI: 10.1021/acs.jced.7b00088.

13 M. Ahmad, K. Manzoor and S. Ikram, Versatile nature of hetero-chitosan based derivatives as biodegradable adsorbent for heavy metal ions; a review, *Int. J. Biol. Macromol.*, 2017, **105**, 190–203, DOI: 10.1016/j.ijbiomac.2017.07.008.

14 M. Ahmad, K. Manzoor, P. Venkatachalam and S. Ikram, Kinetic and thermodynamic evaluation of adsorption of Cu(II) by thiosemicarbazide chitosan, *Int. J. Biol. Macromol.*, 2016, **92**, 910–919, DOI: 10.1016/j.ijbiomac.2016.07.075.

15 P. Z. Ray and H. J. Shipley, Inorganic nano-adsorbents for the removal of heavy metals and arsenic: a review, *RSC Adv.*, 2015, **5**, 29885–29907, DOI: 10.1039/c5ra02714d.

16 A. H. Gedam and R. S. Dongre, Adsorption characterization of Pb(II) ions onto iodate doped chitosan composite: equilibrium and kinetic studies, *RSC Adv.*, 2015, **5**, 54188–54201, DOI: 10.1039/C5RA09899H.

17 H. Hadi Najafabadi, M. Irani, L. Roshanfekr Rad, A. Heydari Haratameh and I. Haririan, Removal of Cu^{2+}, Pb^{2+} and Cr^{6+} from aqueous solutions using a chitosan/graphene oxide composite nanofibrous adsorbent, *RSC Adv.*, 2015, **5**, 16532–16539, DOI: 10.1039/c5ra01500f.

18 M. Yusuf, F. M. Elfghi, S. A. Zaidi, E. C. Abdullah and M. A. Khan, Applications of graphene and its derivatives as an adsorbent for heavy metal and dye removal: a systematic and comprehensive overview, *RSC Adv.*, 2015, **5**, 50392–50420, DOI: 10.1039/c5ra07223a.

19 X. Wang, S. Lü, C. Gao, C. Feng, X. Xu, X. Bai, N. Gao, J. Yang, M. Liu and L. Wu, Recovery of Ammonium and Phosphate from Wastewater by Wheat Straw-based Amphoteric Adsorbent and Reusing as a Multifunctional Slow-Release Compound Fertilizer, *ACS Sustainable Chem. Eng.*, 2016, **4**, 2068–2079, DOI: 10.1021/acssuschemeng.5b01494.

20 T. A. H. Nguyen, H. H. Ngo, W. S. Guo, J. Zhang, S. Liang, Q. Y. Yue, Q. Li and T. V. Nguyen, Applicability of agricultural waste and by-products for adsorptive removal of heavy metals from wastewater, *Bioresour. Technol.*, 2013, **148**, 574–585, DOI: 10.1016/j.biortech.2013.08.124.

21 M. A. Renu, K. Singh, S. Upadhyaya and R. K. Dohare, Removal of heavy metals from wastewater using modified agricultural adsorbents, *Mater. Today: Proc.*, 2017, **4**, 10534–10538, DOI: 10.1016/j.matpr.2017.06.415.

22 W. S. Wan Ngah and M. A. K. M. Hanafiah, Removal of heavy metal ions from wastewater by chemically modified plant wastes as adsorbents: a review, *Bioresour. Technol.*, 2008, **99**, 3935–3948, DOI: 10.1016/j.biortech.2007.06.011.

23 D. Mohan and C. U. Pittman, Arsenic removal from water/wastewater using adsorbents-a critical review, *J. Hazard. Mater.*, 2007, **142**, 1–53, DOI: 10.1016/j.jhazmat.2007.01.006.

24 D. Sud, G. Mahajan and M. P. Kaur, Agricultural waste material as potential adsorbent for sequestering heavy metal ions from aqueous solutions – a review, *Bioresour. Technol.*, 2008, **99**, 6017–6027, DOI: 10.1016/j.biortech.2007.11.064.

 This journal is © The Royal Society of Chemistry 2019

Open Access Article. Published on 11 2019. Downloaded on 2024/7/20 06:15:29.
This article is licensed under a Creative Commons Attribution-NonCommercial 3.0 Unported Licence.

25 D. W. O'Connell, C. Birkinshaw and T. F. O'Dwyer, Heavy metal adsorbents prepared from the modification of cellulose: a review, *Bioresour. Technol.*, 2008, **99**, 6709–6724, DOI: 10.1016/j.biortech.2008.01.036.

26 A. Demirbas, Heavy metal adsorption onto agro-based waste materials: a review, *J. Hazard. Mater.*, 2008, **157**, 220–229, DOI: 10.1016/j.jhazmat.2008.01.024.

27 C. L. Allen, A. R. Chhatwal and J. M. J. Williams, Direct amide formation from unactivated carboxylic acids and amines, *Chem. Commun.*, 2012, **48**, 666–668, DOI: 10.1039/c1cc15210f.

28 M. Monier and A. M. A. El-Sokkary, Modification and characterization of cellulosic cotton fibers for efficient immobilization of urease, *Int. J. Biol. Macromol.*, 2012, **51**, 18–24, DOI: 10.1016/j.ijbiomac.2012.04.019.

29 H. Li, B. Wu, C. Mu and W. Lin, Concomitant degradation in periodate oxidation of carboxymethyl cellulose, *Carbohydr. Polym.*, 2011, **84**, 881–886, DOI: 10.1016/j.carbpol.2010.12.026.

30 N. Gorochovceva and R. Makuška, Synthesis and study of water-soluble chitosan-O-poly(ethylene glycol) graft copolymers, *Eur. Polym. J.*, 2004, **40**, 685–691, DOI: 10.1016/j.eurpolymj.2003.12.005.

31 V. Tangpasuthadol, N. Pongchaisirikul and V. P. Hoven, Surface modification of chitosan films. Effects of hydrophobicity on protein adsorption, *Carbohydr. Res.*, 2003, **338**, 937–942, DOI: 10.1016/S0008-6215(03)00038-7.

32 S. Fujita and N. Sakairi, Water soluble EDTA-linked chitosan as a zwitterionic flocculant for pH sensitive removal of Cu(II) ion, *RSC Adv.*, 2016, **6**, 10385–10392, DOI: 10.1039/c5ra24175h.

33 S. Veeranarayanan, A. C. Poulose, M. Sheikh Mohamed, Y. Nagaoka, S. Iwai, Y. Nakagame, S. Kashiwada, Y. Yoshida, T. Maekawa and D. Sakthi Kumar, Synthesis and application of luminescent single CdS quantum dot encapsulated silica nanoparticles directed for precision optical bioimaging, *Int. J. Nanomed.*, 2012, **7**, 3769–3786, DOI: 10.2147/IJN.S31310.

34 M. D'Halluin, J. Rull-Barrull, G. Bretel, C. Labrugère, E. Le Grognec and F. X. Felpin, Chemically modified cellulose filter paper for heavy metal remediation in water, *ACS Sustainable Chem. Eng.*, 2017, **5**, 1965–1973, DOI: 10.1021/acssuschemeng.6b02768.

35 P. Vijayalakshmi, V. S. S. Bala, K. V. Thiruvengadaravi, P. Panneerselvam, M. Palanichamy and S. Sivanesan, Removal of Acid Violet 17 from Aqueous Solutions by Adsorption onto Activated Carbon Prepared from Pistachio Nut Shell, *Sep. Sci. Technol.*, 2010, **46**, 155–163, DOI: 10.1080/01496395.2010.484006.

36 A. S. K. Kumar, S. Kalidhasan, V. Rajesh and N. Rajesh, Application of cellulose-clay composite biosorbent toward the effective adsorption and removal of chromium from industrial wastewater, *Ind. Eng. Chem. Res.*, 2012, **51**, 58–69, DOI: 10.1021/ie201349h.

37 S. Yang, J. Li, D. Shao, J. Hu and X. Wang, Adsorption of Ni(II) on oxidized multi-walled carbon nanotubes: effect of contact time, pH, foreign ions and PAA, *J. Hazard. Mater.*, 2009, **166**, 109–116, DOI: 10.1016/j.jhazmat.2008.11.003.

38 S. Zhou, A. Xue, Y. Zhao, Q. Wang, Y. Chen, M. Li and W. Xing, Competitive adsorption of Hg^{2+}, Pb^{2+} and Co^{2+} ions on polyacrylamide/attapulgite, *Desalination*, 2011, **270**, 269–274, DOI: 10.1016/j.desal.2010.11.055.

39 M. H. Baek, C. O. Ijagbemi, S. J. O and D. S. Kim, Removal of Malachite Green from aqueous solution using degreased coffee bean, *J. Hazard. Mater.*, 2010, **176**, 820–828, DOI: 10.1016/j.jhazmat.2009.11.110.

40 F. Arias and T. K. Sen, Removal of zinc metal ion (Zn^{2+}) from its aqueous solution by kaolin clay mineral: a kinetic and equilibrium study, *Colloids Surf., A*, 2009, **348**, 100–108, DOI: 10.1016/j.colsurfa.2009.06.036.

41 S. Lagergren, About the theory of so-called adsorption of soluble substances, *K. Sven. Vetenskapsakad. Handl.*, 1898, **24**, 1–39.

42 D. H. K. Reddy, K. Seshaiah, A. V. R. Reddy, M. M. Rao and M. C. Wang, Biosorption of Pb^{2+} from aqueous solutions by *Moringa oleifera* bark: equilibrium and kinetic studies, *J. Hazard. Mater.*, 2010, **174**, 831–838, DOI: 10.1016/j.jhazmat.2009.09.128.

43 W. J. Weber and J. C. Morris, Kinetics of Adsorption on Carbon from Solution, *J. Sanit. Eng. Div., Am. Soc. Civ. Eng.*, 1963, **89**, 31–60, DOI: 10.1073/pnas.85.14.5274.

44 Z. Y. Yao, J. H. Qi and L. H. Wang, Equilibrium, kinetic and thermodynamic studies on the biosorption of Cu(II) onto chestnut shell, *J. Hazard. Mater.*, 2010, **174**, 137–143, DOI: 10.1016/j.jhazmat.2009.09.027.

45 N. Rahman and U. Haseen, Equilibrium modeling, kinetic, and thermodynamic studies on adsorption of Pb(II) by a hybrid inorganic-organic material: polyacrylamide zirconium(IV) iodate, *Ind. Eng. Chem. Res.*, 2014, **53**, 8198–8207, DOI: 10.1021/ie500139k.

46 L. Largitte and R. Pasquier, A review of the kinetics adsorption models and their application to the adsorption of lead by an activated carbon, *Chem. Eng. Res. Des.*, 2016, **109**, 495–504, DOI: 10.1016/j.cherd.2016.02.006.

47 W. S. W. Ngah and S. Fatinathan, Pb(II) biosorption using chitosan and chitosan derivatives beads: equilibrium, ion exchange and mechanism studies, *J. Environ. Sci.*, 2010, **22**, 338–346, DOI: 10.1016/S1001-0742(09)60113-3.

48 A. H. Chen, S. C. Liu, C. Y. Chen and C. Y. Chen, Comparative adsorption of Cu(II), Zn(II), and Pb(II) ions in aqueous solution on the crosslinked chitosan with epichlorohydrin, *J. Hazard. Mater.*, 2008, **154**, 184–191, DOI: 10.1016/j.jhazmat.2007.10.009.

49 S. Chen, Y. Zou, Z. Yan, W. Shen, S. Shi, X. Zhang and H. Wang, Carboxymethylated-bacterial cellulose for copper and lead ion removal, *J. Hazard. Mater.*, 2009, **161**, 1355–1359, DOI: 10.1016/j.jhazmat.2008.04.098.

50 N. Van Suc and H. T. Y. Ly, Lead(II) removal from aqueous solution by chitosan flake modified with citric acid *via* crosslinking with glutaraldehyde, *J. Chem. Technol. Biotechnol.*, 2013, **88**, 1641–1649, DOI: 10.1002/jctb.4013.

51 S. Rajput, L. P. Singh, C. U. Pittman and D. Mohan, Lead (Pb^{2+}) and copper (Cu^{2+}) remediation from water using

Open Access Article. Published on 11 2019. Downloaded on 2024/7/20 06:15:29.
This article is licensed under a Creative Commons Attribution-NonCommercial 3.0 Unported Licence.

superparamagnetic maghemite (γ-Fe_2O_3) nanoparticles synthesized by Flame Spray Pyrolysis (FSP), *J. Colloid Interface Sci.*, 2017, **492**, 176–190, DOI: 10.1016/j.jcis.2016.11.095.

52 N. E. Mousa, C. M. Simonescu, R. E. Pătescu, C. Onose, C. Tardei, D. C. Culiță, O. Oprea, D. Patroi and V. Lavric, Pb^{2+} removal from aqueous synthetic solutions by calcium alginate and chitosan coated calcium alginate, *React. Funct. Polym.*, 2016, **109**, 137–150, DOI: 10.1016/j.reactfunctpolym.2016.11.001.

53 A. Heidari, H. Younesi and Z. Mehraban, Removal of Ni(II), Cd(II), and Pb(II) from a ternary aqueous solution by amino functionalized mesoporous and nano mesoporous silica, *Chem. Eng. J.*, 2009, **153**, 70–79, DOI: 10.1016/j.cej.2009.06.016.

54 A. Afkhami, M. Saber-Tehrani and H. Bagheri, Simultaneous removal of heavy-metal ions in wastewater samples using nano-alumina modified with 2,4-dinitrophenylhydrazine, *J. Hazard. Mater.*, 2010, **181**, 836–844, DOI: 10.1016/j.jhazmat.2010.05.089.

55 X. Guo, B. Du, Q. Wei, J. Yang, L. Hu, L. Yan and W. Xu, Synthesis of amino functionalized magnetic graphenes composite material and its application to remove Cr(VI), Pb(II), Hg(II), Cd(II) and Ni(II) from contaminated water, *J. Hazard. Mater.*, 2014, **278**, 211–220, DOI: 10.1016/j.jhazmat.2014.05.075.

56 L. Chu, C. Liu, G. Zhou, R. Xu, Y. Tang, Z. Zeng and S. Luo, A double network gel as low cost and easy recycle adsorbent: highly efficient removal of Cd(II) and Pb(II) pollutants from wastewater, *J. Hazard. Mater.*, 2015, **300**, 153–160, DOI: 10.1016/j.jhazmat.2015.06.070.

57 D. Liu, Z. Li, W. Li, Z. Zhong, J. Xu, J. Ren and Z. Ma, Adsorption behavior of heavy metal ions from aqueous solution by soy protein hollow microspheres, *Ind. Eng. Chem. Res.*, 2013, **52**, 11036–11044, DOI: 10.1021/ie401092f.

This journal is © The Royal Society of Chemistry 2019